An EGSnrc Monte Carlo-calculated database of TG-43 parameters

R. E. P. Taylor[a] and D. W. O. Rogers[b]
Ottawa Carleton Institute of Physics, Carleton University, Ottawa K1S 5B6, Canada

(Received 18 January 2008; revised 7 April 2008; accepted for publication 14 May 2008; published 25 August 2008)

Monte Carlo methods are used to calculate a complete TG-43 dosimetry parameter data set for 27 low-energy photon emitting brachytherapy sources (18 ^{125}I and 9 ^{103}Pd). All Monte Carlo calculations are performed using the EGSnrc user-code BrachyDose. TG-43 dosimetry parameters, including dose rate constants, radial dose functions (with functional fitting parameters), and anisotropy data, are calculated with finer spatial resolution, greater range of distances, and smaller uncertainties than data currently available in the literature for many of these sources. In particular, for most of the seeds, this is the first time that anisotropy data have been tabulated at distances less than 0.5 cm from the source. These calculations employ the state-of-the-art XCOM photon cross sections, and detailed source geometries are modeled using Yegin's multigeometry package. This data set serves as a completely independent verification of the currently available dosimetry parameters calculated using other Monte Carlo codes, including MCNP and PTRAN. This report also describes the Carleton Laboratory for Radiotherapy Physics TG-43 Parameter Database, a publicly accessible web site (at http://www.physics.carleton.ca/clrp/seed_database/) through which all of the data calculated for this study can be accessed. Also available on the web site are descriptions of the methods and Monte Carlo models used in this study and comparisons of data calculated in this study with data calculated by other authors. [DOI: 10.1118/1.2965360]

Key words: LDR brachytherapy, I-125, Pd-103, EGSnrc, Monte Carlo, database, dose rate constant, radial dose function, anisotropy function

I. INTRODUCTION

The Joint AAPM/RPC Registry of Brachytherapy Sources[1] lists a total of 15 unique low-energy photon emitting brachytherapy sources which comply with the AAPM's requirements for routine clinical use. In order to comply, each seed in the registry requires a full set of TG-43 (Refs. 2–4) dosimetry parameters based on at least one set of measurements and at least one set of Monte Carlo (MC) calculations. TG-43 provides recommendations regarding the spatial resolution and extent of dosimetry parameter data, but authors are free to choose the specific radii and polar angles at which they calculate the TG-43 data, leading to variability in the resolution of available dosimetry data between different source models. Therefore, there is a need to have a complete set of high resolution TG-43 dosimetry data generated at a consistent set of points for all of the registered brachytherapy sources and calculated using state-of-the-art photon cross section data. This data set would facilitate intersource comparisons and could potentially lead to more accurate brachytherapy dosimetry in the clinic. This data set would also be useful in providing a totally independent verification of currently available dosimetry data, most of which has been generated using Williamson's PTRAN code[5,6] or the MCNP Monte Carlo Code.[7]

To generate such a data set, the EGSnrc (Refs. 8 and 9) user-code BrachyDose (Refs. 10–12) is employed to calculate a complete set of TG-43 dosimetry parameters (dose rate constants, radial dose functions, and anisotropy data) for a total of 27 brachytherapy sources (18 ^{125}I and 9 ^{103}Pd) including the 15 sources currently listed in the AAPM/RPC source registry. Data are presented in some cases for seeds which are no longer manufactured to allow for possible retrospective studies and/or to evaluate the accuracy of the data used clinically in the past.

This article outlines the methods used to generate the TG-43 data but, due to the large volume of data, the complete set of dosimetry parameters is not presented here. Instead, only the geometry descriptions and calculated dose rate constants for each source, along with dose rate constants previously reported by other authors are presented in this article. Cases of significant discrepancies between the current and previous calculations are noted. The complete TG-43 dosimetry data set is available via a website which is described in Sec. II.

II. METHODS AND MONTE CARLO MODELS

II.A. Brachytherapy sources

For this study Yegin's multigeometry package[13] is used to model seed geometries with all the detail possible based on the information presented by authors of previous publications. Geometry models include source encapsulation, internal source geometry and the distribution of radioactivity within the source. Descriptions of the source geometries used in this study are provided below and are available with to-scale drawings, as part of the web resource.

II.B. Monte Carlo calculations

The Monte Carlo methods for calculations in this study are described in detail by Taylor *et al.*[12] and as such are only briefly described here. BrachyDose scores the collision kerma per history in a geometric region (voxel) via a track-length estimator. Due to the low energies involved, charged particle equilibrium can be assumed and collision kerma can be considered equal to the absorbed dose to the medium. For the calculations in this study, electrons are not transported and the photon cutoff energy is set to 1 keV. Rayleigh scattering, bound Compton scattering, photoelectric absorption, and fluorescent emission of characteristic x rays are all simulated. All calculations used photon cross sections from the XCOM (Ref. 14) database and mass energy absorption coefficients are calculated using the EGSnrc user-code "g." Photon spectra recommended in TG-43U1 (Ref. 3) are used to sample incident photon energies and probabilities for both ^{125}I and ^{103}Pd. Up to 4×10^{10} histories are simulated in order to reduce the one standard deviation uncertainty (1σ) on the calculated dosimetry parameters to 2% or less for ^{125}I sources and 3% or less for ^{103}Pd sources at a distance of 10 cm from the source.

A recent addition to the development version of EGSnrc makes it possible to use molecular form factors rather than the default independent atom approximation for Rayleigh scattering events in water (personal communication, E. Mainegra-Hing and I. Kawrakaw, National Research Council of Canada). When compared to calculations made with the independent atom approximation, the molecular form factor calculations reveal no statistically significant differences at distances up to 10 cm from the source for both ^{125}I and ^{103}Pd seeds. Since this new (currently undocumented) feature does not appear to cause significant differences in these calculations, the independent atom approximation is used throughout this study. However, we further investigated the sensitivity of these calculations to the inclusion or not of Rayleigh scattering. Calculations were done with Rayleigh scattering turned off and including Compton scattering either with or without the consideration of binding effects. Consistent with earlier results,[15] our results show that it is more accurate to turn off consideration of binding effects in Compton scatter if Rayleigh scattering is not being modeled. However, throughout this study the more accurate model is used, viz. inclusion of Rayleigh scattering and Compton scatter including binding effects.

Dose calculations are done with the source positioned at the center of a rectilinear water phantom (mass density of 0.998 g/cm^3) with dimensions of $30\times30\times30$ cm^3 (effective radius of 18.6 cm). Dose distributions surrounding the source are scored in a three dimensional grid of cubic voxels with TG-43 parameters extracted from the two dimensional plane defined by the seed axis and transverse axis. To take advantage of the simulation symmetry, doses from the four identical quadrants of this plane are averaged. Uncertainties on the average doses are calculated using the approximation that the dose in the voxels from the four quadrants are statistically independent. To minimize the impact of voxel size effects[12,16] while maintaining reasonable efficiency, voxel sizes are chosen in the following way: $0.1\times0.1\times0.1$ mm^3 voxels for distances in the range of $r_{\text{seed}}<r\leq1$ cm, $0.5\times0.5\times0.5$ mm^3 voxels for $1<r\leq5$ cm, and $1\times1\times1$ mm^3 voxels for $5<r\leq10$ cm, where r is defined as the distance from the center of the seed and r_{seed} is the radius of the cylindrical seed encapsulation. Based on Fig. 2 in our previous study[12] the error on dose introduced by voxel size effects at 1 mm distance in a $0.1\times0.1\times0.1$ mm^3 voxel is approximately 0.25% whereas using a voxel size of $0.5\times0.5\times0.5$ mm^3 at the same distance may introduce errors up to 6%.

Calculations of the air kerma per history are scored *in vacuo* avoiding the need to correct for attenuation by air. The mass energy absorption coefficients for air used in this calculation are calculated with the composition recommended by TG-43U1 (40% humidity).[3] Strictly speaking this is incorrect as air kerma is defined in terms of dry air, but the difference in mass energy absorption coefficients for humid and dry air in this energy region is less than 0.01%. Characteristic x rays originating from the titanium encapsulation are suppressed in the air-kerma calculations by discarding photons with energy less than 5 keV (i.e., PCUT is set to 5 keV in EGSnrc).

II.C. TG-43 dosimetry parameters

Dosimetry data are tabulated as a function of distance from the seed and polar angle relative to the seed axis. When tabulation points do not correspond with the center of a voxel (as is usually the case for anisotropy function calculations), dose values are interpolated bilinearly using the nearest neighbors of the voxel that the point of interest falls within. To improve the accuracy of the interpolation, all dose values are first divided by their respective values of the geometry function,[2,3] $G_L(r,\theta)$ which is associated with the voxel's geometric center.

Dose rate constants, Λ, are calculated by dividing the dose-to-water per history in a (0.1 mm)^3 voxel centered on the reference position in the $30\times30\times30$ cm^3 water phantom $(1\text{ cm},\pi/2)$, by the air-kerma strength per history (scored *in vacuo*). Williamson *et al.*,[17–19] Lymperopoulou *et al.*,[20] and our group[12] have previously shown that for some sources, calculated air-kerma strength depends on the size of the scoring region used. For this reason dose rate constants are provided for air-kerma strengths calculated using voxel sizes of $2.7\times2.7\times0.05$ cm^3 and $0.1\times0.1\times0.05$ cm^3 located on the transverse axis 10 cm from the source (as described in our previous study[12]). The larger voxel size averages the air kerma per history over a region covering roughly the solid angle subtended by the primary collimator of the NIST Wide Angle Free Air Chamber (WAFAC).[21,22] The small voxel serves to estimate the air kerma per history at a point on the transverse axis. These two voxel sizes are referred to as WAFAC and point voxels in the remainder of this article.

The radial dose function $g(r)$ is calculated using both line and point source geometry functions and tabulated at intervals of 0.01 cm for $0.05\leq r\leq0.1$ cm, 0.1 cm for

$0.1 < r \leqslant 1.0$ cm, and 0.5 cm for $5 < r \leqslant 10$ cm. Values at $r=0.15$, 0.25, and 0.75 cm are also included. Anisotropy functions, $F(r,\theta)$, are calculated using the line source approximation for all sources and tabulated at radii of 0.1, 0.15, 0.25, 0.5, 0.75, 1, 2, 3, 4, 5, 7.5, and 10 cm and 32 polar angles with a minimum resolution of 5°. For most of the seeds, this study is the first to report anisotropy function data at distances less than 0.5 cm from the source which may be of particular interest in eye plaque brachytherapy treatments. The anisotropy factor $\phi_{an}(r)$ is calculated by integrating the solid-angle-weighted dose rate over $0° \leqslant \theta \leqslant 90°$.

III. DETAILED SOURCE DESCRIPTIONS

This section gives a detailed description of each source modeled in our Monte Carlo calculations with Yegin's multigeometry package.[13] Scale drawings of each seed are available via Sec. V. Empty space in all of the seeds listed below is assumed to be filled with air. Since most of the seeds have source and marker elements which are free to move within their encapsulation, a rough estimate of the possible extent of this movement is also provided. The extent of movement of source elements can be used to provide a rough estimate of one component of geometric uncertainty in dose calculations and is discussed further in Sec. IV A.

III.A. ^{125}I sources

III.A.1. Amersham, OncoSeed, 6702

Dimensions given in the article by Williamson and Quintero[24] are used for the 6702 source[5,24–28]. The 6702 source consists of three resin spheres (resin density is 1.2 g/cm^3 and has a molecular composition[24] of $C_{12}H_{18}NCl$), each with a diameter of 0.600 mm. The spheres are coated with ^{125}I which is assumed to have negligible thickness in this study. The spheres are encapsulated in a titanium tube with 0.050 mm thick walls and an outer diameter of 0.800 mm and length of 3.50 mm. End welds are 0.500 mm thick and are modelled as 0.400 mm hemispheres on top of solid cylinders that have a 0.400 mm radius and are 0.100 mm thick. The overall length is 4.50 mm and the active length in this study was 3.30 mm (calculated using the TG-43 effective line source length with a seed spacing of 1.10 mm and $N=3$ sources). The maximum possible displacement of a source sphere from its nominal position is 1.45 mm along the seed axis and 0.050 mm in the radial direction.

III.A.2. Amersham, OncoSeed, 6711

Source dimensions for the 6711 seed[5,23] are taken from the article by Dolan *et al.*[23] which presents a more realistic geometry than has been used in previous studies. The 6711 source consists of radioactive AgI and AgBr (Ref. 23) (2.5:1 molecular ratio of AgI:AgBr and a density of 6.2 g/cm^3) coated on a 2.80 mm long cylindrical silver rod with a 0.250 mm radius. The ends of the silver rod are conical sections beveled at 45.0° and the end faces of the rod have a radius of 0.175 mm. The radioactive coating is assumed to have a thickness of 1.75 μm over the entire surface of the rod. The silver rod is encapsulated in a 3.75 mm long titanium tube with 0.0700 mm thick walls, a 0.800 mm outer diameter, and 0.375 mm thick hemispherical end welds. The overall source length is 4.55 mm and the active length is 2.80 mm. The cylindrical source element is free to move 0.475 mm along the seed axis and 0.080 mm radially from the center of the seed.

III.A.3. Amersham, EchoSeed, 6733

Dimensions for the 6733 seed[29,30] are taken from the study by Sowards and Meigooni.[29] The 6733 source consists of ^{125}I coated on a 3.00 mm long cylindrical silver rod which is 0.250 mm in radius. In this study the ^{125}I coating is assumed to have a thickness of 2.00 μm on both the cylindrical surface and end faces. The silver rod is encapsulated in a titanium tube with 0.050 mm thick walls, 0.800 mm outer diameter, and 0.500 mm thick end welds. End welds are modeled using a 0.400 mm Ti hemisphere overlapped with a 0.350 mm air sphere with its center shifted by 0.250 mm relative to the Ti sphere. The titanium casing is unique in that it is "threaded" with six threads. In this study the threads are taken to be a series of 11 0.050 mm thick cylindrical shells each approximately 0.332 mm wide and spaced evenly over the central 3.00 mm of the seed. To create the threads, every other cylindrical shell is indented 0.250 mm from the outer cylinders (i.e., the inner threads have inner and outer radii of 0.325 and 0.375 mm, respectively). The overall source length is 4.50 mm and the active length is 3.00 mm. The cylindrical source element is free to move from the nominal position by approximately 0.350 mm along the seed axis and 0.065 mm in the radial direction.

III.A.4. Bacon Co., Braquibac

Dimensions for the Braquibac source[31] are taken from the study by Pirchio *et al.*[31] The source element for the Braquibac seed is a cylindrical silver rod with an outer diameter of 0.500 mm and a length of 3.07 mm. The rod is coated with a silver halide layer that is 1.00 μm thick. The titanium encapsulation has a 0.779 mm outer diameter and is 0.090 mm thick. End welds are 0.390 mm thick and approximated here as being hemispherical in shape. The overall source length is 4.68 mm and the active length of the source is 3.07 mm. The cylindrical source element is free to move 0.415 mm along the seed axis and 0.064 mm radially from the center of the seed.

III.A.5. BEBIG GmbH, IsoSeed, I25.S06 / Theragenics, I-Seed, I25.S06

Seed dimensions for the I125.S06 seed[32,33] are taken from the article by Hedtjärn *et al.*[32] This source consists of ^{125}I uniformly distributed throughout a hollow cylindrical alumina (Al_2O_3) core with inner and outer diameters of 0.220 and 0.600 mm, respectively. For the purpose of these calculations the amount of ^{125}I present in the alumina is assumed to be negligible. Within the hollow core is a 0.350 mm long

gold rod with a diameter of 0.170 mm. The core is encapsulated in a titanium tube with 0.050 mm thick walls and 0.800 mm outer diameter. The end welds are slightly concave and have a thickness of 0.440 mm in the middle. End welds are modeled using a 0.400 mm Ti hemisphere overlapped with a 0.889 mm air sphere with its center shifted by 0.969 mm relative to the Ti sphere. The overall source length is 4.56 mm and the active length is 3.50 mm. The cylindrical source element is free to move roughly 0.110 mm along the seed axis and 0.050 mm radially from the center of the seed.

III.A.6. BEBIG GmbH, IsoSeed, I25.S17

The IsoSeed I125.S17 (Refs. 20 and 34) source dimensions are taken from the study by Lymperopoulou *et al.*[20] The source element for the IsoSeed is a cylindrical molybdenum rod with an outer diameter of 0.500 mm and a length of 3.40 mm. The rod is coated with a layer of nickel that is 3.00 μm thick. On top of the nickel is a 25.0 μm thick layer of silver which is in turn coated with a 2.00 μm thick layer of radioactive silver iodide. The titanium encapsulation has a 0.800 mm outer diameter and is 0.050 mm thick. End welds are 0.400 mm thick and hemispherical in shape. The overall source length is 4.5 mm and the active length of the source is 3.46 mm. The cylindrical source element is free to move 0.120 mm along the seed axis and 0.070 mm radially from the center of the seed.

III.A.7. Best Industries Best I-125 2301

Dimensions for the Best 2301 source[35–37] are taken from the study by Sowards and Meigooni.[35] The 2301 source consists of a cylindrical tungsten marker 3.75 mm long with a diameter of 0.250 mm. In this study the ends of the marker are assumed to be round as shown in the figure in TG-43U1.[3] The marker is coated with an organic matrix (assumed to be polystyrene with a density of 1.06 g/cm^3 and a composition by weight of 7.74% H and 92.3% C) containing ^{125}I. For the purpose of these calculations the amount of ^{125}I present in the polystyrene is assumed to be negligible. The thickness of the coating is assumed to be 0.100 mm on the cylindrical surface as well as the round ends. The active element is encapsulated in a 0.080 mm thick titanium casing with an outer diameter of 0.800 mm. The end welds are assumed to be hemispherical shells with a thickness of 0.080 mm. The overall source length is 5.00 mm and the active length is 3.95 mm. The cylindrical source element is free to move approximately 0.445 mm along the seed axis and 0.0950 mm radially from the center of the seed.

III.A.8. DRAXIMAGE, BrachySeed, LS-1

Seed dimensions for the LS-1 seed[38–42] are the same as those used in the study by Williamson.[38] The DRAXIMAGE BrachySeed LS-1 consists of two 0.500 mm diameter aluminum silicate spheres containing a uniform distribution of ^{125}I. Density of the aluminum silicate is 2.81 g/cm^3 and composition by weight is 40.7% O, 21.4% Si, 16.6% Al, 11.3% Na, and 10.0% Ag[38] (the amount of ^{125}I within the spheres is assumed to be negligible). The two source spheres are separated by a 90% Pt/10% Ir cylindrical rod that is 3.00 mm long and has a diameter of 0.380 mm. At the middle of the seed is a 1.20 mm long Ti annulus with inner and outer diameters of 0.390 and 0.698 mm, respectively. The wall thickness of the cylindrical portion of the source is 0.100 mm. The hemispherical ends are 0.065 mm thick on the longitudinal axis and 0.050 mm thick where they meet the cylindrical walls. End welds are modeled using a 0.400 mm radius Ti hemisphere overlapped with a 0.350 mm radius air sphere with its center shifted by 0.015 mm relative to the Ti sphere. The overall source length is 4.40 mm and the active length is 4.10 mm which is the physical extent of the activity distribution within the source. The two spheres are free to move approximately 0.050 mm along the seed axis and 0.050 mm radially.

III.A.9. IBt, InterSource, 1251L

Dimensions for the InterSource seed[43,44] are taken from the study by Meigooni *et al.*[43] The InterSource consists of two concentric hollow titanium cylindrical tubes which are laser welded together at the ends. Each tube is 0.040 mm thick and the outer diameter of the inner and outer tubes are 0.500 and 0.810 mm, respectively. There is a thin band (0.045 mm thick and 1.27 mm long) of 90% Pt/10% Ir alloy deposited on top of the inner cylinder at its center. The radioactive ^{125}I is distributed uniformly throughout three cylindrical bands of an organic material (85.7% C 14.3% H with a density of 1.00 g/cm^3 in which the ^{125}I content is assumed to be negligible). The outer two bands of radioactive material are deposited on the inner cylinder and are 0.800 mm long, 0.015 mm thick and have their centers along the seed axis offset 1.45 mm from the middle of the seed. The center band is 0.500 mm long, 9.00×10^{-3} mm thick and is deposited on top of the Pt/Ir alloy. The overall length is 4.5 mm and the active length of the seed is 4.35 mm.[45]

III.A.10. Imagyn, IsoStar, IS-12501

Dimensions given in the article by Gearheart *et al.*[46] are used for the Imagyn source.[12,46–49] The Imagyn source consists of five silver spheres, each with a diameter of 0.640 mm, coated with AgI and encapsulated in a titanium tube with 0.500 mm thick end welds. The end welds are modeled as 0.400 mm hemispheres on top of solid cylinders that have a 0.400 mm radius and are 0.100 mm thick. The center of the spheres are along the seed axis offset 0.690 mm from each other. The tube has 0.050 mm thick walls and an outer diameter of 0.800 mm. The AgI coating is assumed to have negligible thickness in this study. The overall length is 4.50 mm and the active length is 3.40 mm. The maximum possible displacement of a source sphere is 0.350 mm along the seed axis as well as up to 0.030 mm in the radial direction.

III.A.11. Implant Sciences Corp., IPlant, 3500

Dimensions for the I-Plant seed[50–53] are taken from the study by Rivard.[50] The I-Plant seed has a Ti capsule with an outside diameter of 0.836 mm and end welds which are

0.330 mm thick spherical sections. The end welds are modeled using a 0.225 mm thick section of a 0.500 mm radius Ti sphere attached to a 0.105 mm thick Ti cylinder with a radius of 0.418 mm. The wall thickness of the Ti capsule is 0.0558 mm. Inside the source there is a Ag marker assumed to have a total length of 3.60 mm and a radius of 0.200 mm. The conical ends of the marker have a half-angle of approximately 18°. The active element of the source is a quartz tube surrounding the marker that is 3.76 mm in length with inside and outside diameters of 0.432 and 0.635 mm, respectively. The quartz tube is covered in a 16.0 μm thick active layer of Si containing ^{124}Xe which is in turn covered by a 5.00 μm thick layer of SiO_2. The active layer is assumed to have a density of 2.58 g/cm^3 and is composed of 97.6% Si, 2.38% Xe, 1.60×10^{-3}% I, and 6.00×10^{-4}% Te.[50] The overall length is 4.60 mm and the active length is 3.76 mm. The cylindrical source element is free to move approximately 0.090 mm along the seed axis and 0.056 mm radially from the center of the seed.

III.A.12. IsoAid, LLC, Advantage, IAI-125A

Dimensions for the IAI-125A source[54,55] are taken from the study by Meigooni *et al.*[54] The IsoAid Advantage seed contains a 3 mm long silver rod with a diameter of 0.500 mm. The silver rod is coated with a 1 μm thick layer of AgI containing ^{125}I (coating assumed to be the same thickness on the cylindrical and end face surfaces). The source is encapsulated in a titanium casing 0.050 mm thick with an outside diameter of 0.800 mm. The end welds have a maximum thickness of 0.100 mm and are modeled using a 0.400 mm radius Ti hemisphere overlapped with a 0.350 mm radius air sphere with its center shifted laterally inward by 0.050 mm relative to the Ti sphere. The overall source length is 4.50 mm and the active length is 3.00 mm. The cylindrical source element is free to move approximately 0.350 mm along the seed axis and 0.100 mm radially from the center of the seed.

III.A.13. Mills Biopharmaceuticals, LLC, ProstaSeed, 125SL

Dimensions and internal source positions for the ProstaSeed source[56,57] are taken from the nominal configuration in the study by Li.[56] The ProstaSeed contains five silver spheres (0.500 mm diameter) which are coated in ^{125}I. As in the study by Li[56] the ^{125}I is assumed to be of negligible thickness. The five spheres are free to move within the Ti encapsulation which has an outer diameter of 0.800 mm and has walls with a thickness of 0.050 mm and 0.300 mm thick end welds. The end welds are modeled using a 0.400 mm radius Ti hemisphere overlapped with a 0.350 mm radius air sphere with its center shifted laterally inward by 0.250 mm relative to the Ti sphere. The overall length is 4.50 mm and the active length is 3.00 mm. The maximum possible displacement of a source sphere is 0.850 mm along the seed axis and 0.100 mm in the radial direction.

III.A.14. North American Scientific, Prospera I-125, Med 3631-A/M

Dimensions and internal source configurations for the Med3631 source[58–60] are taken from the study by Rivard.[58] The Med3631 ^{125}I seed consists of polystyrene spheres (0.560 mm diameter), coated with a negligible thickness of radioactive material, with two located on each side of two 0.560 mm diameter 80% Au/20% Cu alloy spheres. The encapsulating titanium cylinder has an outside diameter of 0.810 mm and an inner diameter of 0.710 mm. The source has an average weld thickness of 0.100 mm. The end welds are modeled using a 0.405 mm radius Ti hemisphere overlapped with a 0.355 mm radius air sphere with its center shifted by 0.050 mm relative to the Ti sphere. Calculations are done with the internal spheres arranged in the "ideal" configuration (center of source spheres located at $\pm$1.807 mm and $\pm$1.084 mm, center of marker spheres located at $\pm$0.361 mm) given in the study of the Med3631 ^{125}Iseed by Rivard.[58] Rivard's study also contains a discussion on how the internal movement of the source spheres effects dosimetry parameters. The overall length is 4.70 mm and the active length is assumed to be 4.20 mm.

III.A.15. Nucletron, SelectSeed I-125, 130.002

The SelectSeed source[61–63] dimensions are taken from the study by Karaiskos *et al.*[61] The source element for the SelectSeed is a cylindrical silver rod with an outer diameter of 0.510 mm and a length of 3.40 mm. The rod is coated with a silver halide layer (AgCl/AgI) that is 3.00 μm thick. The titanium encapsulation has a 0.800 mm outer diameter and is 0.050 mm thick. End welds are 0.400 mm thick and hemispherical in shape. The overall length is 4.50 mm and the active length of the source is 3.40 mm. The cylindrical source element is free to move approximately 0.147 mm along the seed axis and 0.092 mm radially from the center of the seed.

III.A.16. Bard Urological Division, 125 Implant Seed, STM1251

The dimensions used by Kirov and Williamson[18] in their study of the STM seed[12,18,64,65] are used here. The STM1251 source consists of a cylindrical gold rod (0.180 mm diameter) inside of a 3.81 mm long hollow aluminum wire with a diameter of 0.510 mm. The aluminum wire is coated with 1.90 μm of nickel, 2.50 μm of copper, and 17.0 nm of radioactive iodine. The coating is assumed to cover the end faces of the aluminum wire and gold rod. The source is encapsulated in a titanium tube with 0.080 mm thick walls, 0.810 mm outer diameter, and 0.130 mm thick solid cylindrical end welds. The overall source length is 4.50 mm and the active length is 3.80 mm. The cylindrical source element is free to move 0.240 mm along the seed axis and 0.066 mm radially from the center of the seed.

III.A.17. Syncor, PharmaSeed, BT-125-1 and BT-125-2

The PharmaSeed BT-125-1 source[55,66,67] dimensions are taken from the study by Popescu *et al.*.[66] The source element for the PharmaSeed BT-125-1 is a cylindrical palladium rod with an outer diameter of 0.500 mm and a length of 3.25 mm. The rod is coated with a 0.500 μm thick layer of ^{125}I. The titanium encapsulation has a 0.800 mm outer diameter and is 0.060 mm thick. End welds are 0.500 mm thick and are modeled as 0.400 mm hemispheres on top of solid cylinders that are 0.100 mm thick and have a 0.400 mm radius. The BT-125-2 source[55,67] is the same as the BT-125-1 source with the exception that the cylindrical rod is made of Ag rather than Pd. The overall source length is 4.50 mm and the active length of both sources is 3.25 mm. The cylindrical source element can move 0.124 mm along the seed axis and 0.090 mm radially from the center of the seed.

III.B. ^{103}Pd Sources

III.B.1. BEBIG GmbH, IsoSeed, ^{103}Pd

Seed dimensions for the BEBIG GmbH ^{103}Pd seed are taken from the article by Daskalov and Williamson.[68] This source consists of ^{103}Pd uniformly distributed throughout a 3.50 mm long hollow cylindrical alumina (Al_2O_3) core with inner and outer diameters of 0.250 and 0.600 mm, respectively. For the purpose of these calculations the amount of ^{103}Pd present in the alumina is assumed to be negligible. Within the core is a 3.50 mm long gold rod with a diameter of 0.200 mm. The core is encapsulated in a titanium tube with 0.050 mm thick walls and 0.800 mm outer diameter. The end welds are slightly concave and have a thickness of 0.435 mm in the middle. End welds are modeled using a 0.400 mm Ti hemisphere overlapped with a 0.806 mm radius air sphere with its center shifted by 0.846 mm relative to the Ti sphere. The overall source length is 4.56 mm and the active length is 3.50 mm. The cylindrical source element is free to move 0.050 mm radially and a negligible amount along the seed axis.

III.B.2. Best Industries, Best Palladium-103, 2335

Dimensions for the 2335 source[69,70] are taken from studies by Meigooni *et al.*[69] and Peterson and Thomadsen.[70] The Best 2335 source consists of a cylindrical tungsten marker which is 1.20 mm long with a diameter assumed to be approximately 0.500 mm. On either side of the marker are three 0.560 mm diameter spheres located 0.900, 1.50, and 2.10 mm from the middle of the seed. The spheres are made of a polymer (composition by weight[69] of 89.7% C, 7.85% H, 1.68% O, and 0.740% N, and density of the polymer is assumed to be 1.00 g/cm^3). The polymer spheres are coated in ^{103}Pd which is assumed to have negligible thickness. The spheres and titanium marker are encapsulated with the same Ti casing described above for the Best 2301 ^{125}I source. The overall source length is 5.00 mm and the active length was taken to be 4.76 mm, the extent of the activity distribution within the source. The maximum possible displacement of a source sphere is 0.570 mm along the seed axis and up to 0.070 mm in the radial direction.

III.B.3. DRAXIMAGE, BrachySeed, Pd-1

The source dimensions for the Pd-1 seed[71–73] are taken from the study by Chan and Prestwich.[73] The DRAXIMAGE BrachySeed Pd-1 source consists of two 0.55 mm diameter aluminum silicate spheres containing a uniform distribution of ^{103}Pd (spheres have a density of 2.53 g/cm^3 and the composition by weight[73] is 45.2% O, 23.8% Si, 18.4% Al, and 12.6% Na with a negligible amount of ^{103}Pd). The two source spheres are separated by a 90% Pt/10% Ir cylindrical rod that is 3.10 mm long and has a diameter of 0.380 mm. At the middle of the seed is a 1.19 mm long Ti annulus with inner and outer diameters of 0.380 mm and 0.691 mm, respectively. On either side of the annulus are two 1.19 mm long cylindrical Ti spacers with inner and outer diameters of 0.589 and 0.691 mm, respectively. These components are encapsulated in a 0.051 mm thick Ti capsule that is 3.60 mm long and has an outside diameter of 0.800 mm. The hemispherical ends are 0.065 mm thick on the longitudinal axis and 0.0500 mm thick where they meet the cylindrical walls. The end welds are modeled using a 0.400 mm radius Ti hemisphere overlapped with a 0.349 mm radius air sphere with its center shifted by 0.0565 mm relative to the Ti sphere. The overall source length is 4.40 mm and the active length is 4.20 mm, the extent of the activity distribution within the seed. The two spheres are free to move approximately 0.050 mm along the seed axis and 0.050 mm radially from the center of the seed.

III.B.4. IBt, InterSource, 1031L

The materials and dimensions for the ^{103}Pd InterSource[74] are the same as those of the ^{125}I InterSource[43,44] presented above, with the exception of ^{125}I being replaced with ^{103}Pd.

III.B.5. IBt, OptiSeed, 1032P

The dimensions for the OptiSeed[75,76] are taken from the study by Bernard and Vynckier.[75] Encapsulation for the OptiSeed is made of biocompatible polymer (the exact polymer is unknown and assumed to be polyethylene) with inner and outer diameters of 0.400 and 0.800 mm, respectively. The ends are sealed with a 0.600 mm long cylindrical piece of polymer (diameter 0.400 mm). The ends are formed into spherical "cups." In this study the cups are assumed to be air filled spheres that are 0.400 mm in diameter and have their centers shifted 2.35 mm from the center of the source. Directly adjacent to the end cups are 0.700 mm long and 0.400 mm diameter polymer cylinders (assumed to be polystyrene) with ^{103}Pd uniformly distributed throughout. The amount of ^{103}Pd present in the polymer is assumed to be negligible. At the center of the source there is a 2.00 mm long Au cylinder with an outer diameter just larger than the inner diameter of the polymer tube (the gold marker is assumed to have a diameter of 0.450 mm). The space between the polymer cylinders and Au marker is assumed to be air.

The overall source length is 5.00 mm and the active length of 3.80 mm is the physical extent of the activity distribution within the source.

III.B.6. IsoAid, Advantage Pd-103, IAPd-103A

Dimensions for the Advantage Pd-103 source[77,78] are from the study by Meigooni *et al.*[77] The IsoAid Advantage ^{103}Pd seed contains four spherical polystyrene beads with a diameter of 0.500 mm. The ^{103}Pd for this source is assumed to be distributed uniformly throughout the volume of the four beads. The four beads are separated into two pairs by a cylindrical silver marker that is 0.500 mm in diameter and 1.25 mm long. The centers of the two beads within a pair are offset 0.968 and 1.56 mm. The source is encapsulated in a titanium casing 0.050 mm thick with an outside diameter of 0.800 mm. The end welds have a maximum thickness of 0.350 mm and are modeled using a 0.405 mm radius Ti hemisphere overlapped with a 0.890 mm radius air sphere with its center shifted by 0.840 mm relative to the Ti sphere. The overall source length is 4.50 mm and the active length is 3.62 mm which is the physical extent of radiation within the source. The maximum possible displacement of a source sphere is 0.459 mm along the seed axis and up to 0.070 mm in the radial direction.

III.B.7. North American Scientific, Prospera Pd-103,Med 3633-A/M

Dimensions for the Med3633 seed[79,80] are taken from the study by Rivard.[79] The Med3633 ^{103}Pd seed consists of two polystyrene spheres (0.560 mm diameter), coated with a negligible thickness of radioactive material, located on either side of two 0.560 mm diameter 80.0% gold/20.0% copper alloy spheres. The encapsulating titanium cylinder has an outer diameter of 0.810 mm and an inner diameter of 0.710 mm. The source has an average weld thickness of 0.100 mm. Calculations are done with the internal spheres arranged in the ideal configuration (center of source spheres located at ± 1.807 and ± 1.084 mm, center of marker spheres located at ± 0.361 mm) given in the study of the Med3631 ^{125}I seed by Rivard.[58] Rivard's study of the Med3631 also contains a discussion on how the internal movement of the source spheres effects dosimetry parameters. The overall length is 4.70 mm and the active length is assumed to be 4.20 mm.

III.B.8. Syncor, PharmaSeed, BT-103-3

Dimensions for the PharmaSeed BT-103-3 are taken from the study by DeMarco *et al.*[67] The Syncor BT-103-3 ^{103}Pd contains four spherical polystyrene beads with a diameter of 0.550 mm. The polystyrene beads are coated in 0.500 μm of ^{103}Pd. The beads are separated into two pairs by a cylindrical gold marker that is 0.500 mm in diameter and 1.10 mm long. The source is encapsulated in a Ti casing 0.050 mm thick with an outside diameter of 0.800 mm. The end welds have a maximum thickness of 0.240 mm and are modeled using a 0.400 mm radius Ti hemisphere overlapped with a 0.350 mm radius air sphere whose center is shifted 0.190 mm relative to the Ti sphere. The overall source length is 4.50 mm and the active length used in our model is 3.75 mm, the physical extent of the activity distribution within the source. The maximum possible displacement of a source sphere is 0.585 mm along the seed axis and 0.075 mm in the radial direction.

III.B.9. Theragenics Corporation, TheraSeed, 200

Dimensions for the TheraSeed[12,17,19,81] are as reported by Monroe and Williamson.[19] The TheraSeed consists of two cylindrical graphite pellets coated with radioactive palladium and separated by a cylindrical lead marker. The graphite cylinders have a diameter of 0.560 mm and length of 0.890 mm. The lead marker is 1.09 mm long and 0.500 mm in diameter. The thickness of Pd on the graphite is 2.20 μm. Encapsulation for the TheraSeed is a thin titanium tube that has an outer diameter of 0.826 mm with wall thickness of 0.056 mm. The ends are sealed with two titanium end cups that are 0.040 mm thick. The end cups are composed of a 0.334 mm long hollow cylindrical section attached to a hemispherical shell. Both the cylindrical section and hemispherical shell have inner diameters of 0.306 mm. The overall source length is 4.500 mm and the active length is 4.23 mm calculated using the TG-43 effective line source length approximation. The maximum displacement of one of the cylindrical sources is 0.200 mm along the seed axis and 0.075 mm in the radial direction.

IV. RESULTS

Due to the large amount of data generated during this study only the dose rate constants calculated in this study and by other authors are presented here. The entire TG-43 dosimetry data set is available at the website described in the Sec. V and fits to the radial dose functions, $g(r)$, are presented in our accompanying study.[82] While the raw $g(r)$ data are first normalized so that $g(r=1\text{ cm})=1.000$, this gives undue importance to the single calculated dose value at $r=1$ cm. Using the fits presented in the accompanying study, the $g(r)$ data for each seed are renormalized by dividing by the initial fitted value of $g(r)$ at 1 cm. By doing this, after fitting to the renormalized data, the fitted value of $g(r)$ at 1 cm is exactly 1.000. In essence, this uses all of the $g(r)$ data equally in normalizing the curve and results in the fitted value of $g(r=1\text{ cm})$ being 1.000 as given by the definition of $g(r)$. Another consequence is that the renormalized individual data point at $g(r=1\text{ cm})$ may no longer be 1.000 (although it is always within 0.4% of unity).

Calculated dose rate constants and their statistical uncertainties are listed in Tables I (^{125}I) and II (^{103}Pd). As mentioned previously, dose rate constants are calculated using values of air kerma scored in large (WAFAC) and small (point) voxels. For most sources the WAFAC and point-voxel dose rate constants are the same within calculated statistical uncertainties. However, for sources with solid cylinders coated with radioactive material, the values of the dose rate constant can vary by up to 5% depending on the size of voxel used for scoring air kerma. Dose rate constants calcu-

TABLE I. Dose rate constants and uncertainties calculated in this study and by other authors for ^{125}I sources. Uncertainties shown for values calculated in this study are statistical uncertainties only and do not include uncertainties in cross sections or geometry. Monte Carlo dose rate constants are generally evaluated with air-kerma strengths calculated by one of three different methods: at a point on the transverse axis, the extrapolation method of Williamson (see Ref. 17) or a scoring geometry approximating the WAFAC at NIST (see Refs. 21 and 22). In the following table these three methods are referred to as point, extrap. and WAFAC, respectively. Air-kerma calculations in this study are made with two voxel sizes located 10 cm from the source on the transverse axis: "WAFAC" ($2.7\times2.7\times0.05$ cm^3) and "point" ($0.1\times0.1\times0.05$ cm^3). Dose rate constants calculated using an approximation of the WAFAC geometry are likely the most clinically relevant.

Manufacturer and seed name	Reference	Method	Λ cGy h^{-1} U^{-1}
Amersham	This study	WAFAC	1.000 ± 0.004
OncoSeed	This study	Point	1.003 ± 0.003
6702	32	Extrap. (PTRAN)	1.016
	26	Point (EGS4)	1.009
	3	Consensus value	1.036
Amersham	This study	WAFAC	0.924 ± 0.002
OncoSeed	This study	Point	0.942 ± 0.003
6711	23	PTRAN (WAFAC)	0.942 ± 0.017
	23	TLD	0.971 ± 0.059
	3	Consensus value	0.965
Amersham	This study	WAFAC	0.929 ± 0.002
EchoSeed	This study	Point	0.947 ± 0.003
6733	29	Point (PTRAN)	0.97 ± 0.03
	30	TLD	0.99 ± 0.08
	4	Consensus value	0.980
Bacon Co.	This study	WAFAC	0.917 ± 0.003
Braquibac	This study	Point	0.949 ± 0.003
	31	Extrap. (MCNP)	0.937 ± 0.004
BEBIG GmbH/	This study	WAFAC	1.011 ± 0.002
Theragenics	This study	Point	1.016 ± 0.003
IsoSeed	32	Extrap. (PTRAN)	1.002
I25.S06	33	TLD	1.033 ± 0.066
	3	Consensus value	1.012
BEBIG GmbH	This study	WAFAC	0.916 ± 0.002
IsoSeed	This study	Point	0.941 ± 0.003
I25.S17	20	Point (MCNP)	0.944 ± 0.014
	20	WAFAC (MCNP)	0.914 ± 0.014
	20	TLD	0.951 ± 0.044
Best Medical	This study	WAFAC	0.998 ± 0.002
Best I-125	This study	Point	1.002 ± 0.003
2301	35	Point (PTRAN)	1.01 ± 0.03
	36	TLD	1.01 ± 0.08
	37	TLD	1.02 ± 0.07
	3	Consensus value	1.018
DRAXIMAGE	This study	WAFAC	0.922 ± 0.002
BrachySeed	This study	Point	0.922 ± 0.005
LS-1	38	WAFAC (PTRAN)	0.935 ± 0.017
	39	Point (EGS4)	0.932 ± 0.003
	42	TLD	1.02 ± 0.07
	40	GaFfilm	0.98 ± 0.06
	40	Extrap (CYLTRAN)	0.90 ± 0.03
	4	Consensus value	0.972
IBt	This study	WAFAC	0.992 ± 0.001
InterSource	This study	Point	0.995 ± 0.003
1251L	43	Point (PTRAN)	1.013 ± 0.03
	43	TLD	1.014 ± 0.08
	44	Point (MCNP)	1.02 ± 0.01
	44	TLD	1.05 ± 0.07
	4	Consensus value	1.038
Imagyn	12	WAFAC	0.924 ± 0.003
IsoStar	12	Point	0.923 ± 0.003
IS-12501	49	Point (PTRAN)	0.92
	46 and 48	TLD	0.92 ± 0.07
	47	TLD	0.95 ± 0.095
	3	Consensus value	0.940
Implant Sciences	This study	WAFAC	0.994 ± 0.002
IPlant	This study	Point	0.998 ± 0.003
3500	50	Extrap. (MCNP)	1.017 ± 0.005
	53	TLD	1.01 ± 0.04
	52	TLD	1.01
	4	Consensus value	1.014
IsoAid.	This study	WAFAC	0.925 ± 0.002
Advantage	This study	Point	0.959 ± 0.002
IAI-125A	54	Point (PTRAN)	0.98 ± 0.03
	54	TLD	0.99 ± 0.08
	55	Point (MCNP)	0.962 ± 0.005
	55	TLD	0.96 ± 0.05
	4	Consensus value	0.981
Mills Bio. Pharm.	This study	WAFAC	0.930 ± 0.002
ProstaSeed	This study	Point	0.932 ± 0.003
125SL	56	Point (PTRAN)	0.925 ± 0.04
	57	TLD	0.980 ± 0.03
	4	Consensus value	0.953
NASI	This study	WAFAC	0.978 ± 0.003
Prospera I-125	This study	Point	0.977 ± 0.003
Med3631	58	Point (MCNP)	1.011 ± 0.03
	59	TLD	1.067
	60	TLD	1.056
	3	Consensus value	1.036
Nucletron	This study	WAFAC	0.917 ± 0.002
SelectSeed	This study	Point	0.944 ± 0.003
130.002	61	MC	0.954 ± 0.005
	62	TLD	0.938 ± 0.065
	63	TLD	0.987 ± 0.077

TABLE I. (*Continued.*)

Manufacturer and seed name	Reference	Method	Λ cGy h^{-1} U^{-1}
STM	12	WAFAC	1.012 ± 0.002
Implant	12	Point	1.045 ± 0.003
STM1251	18	WAFAC (PTRAN)	0.980 ± 0.024
	18	Extrap (PTRAN)	1.041 ± 0.024
	65	TLD	1.039 ± 0.073
	64	TLD	1.07 ± 0.06
	4	Consensus value	1.018
Syncor	This study	WAFAC	0.901 ± 0.002
PharmaSeed	This study	Point	0.938 ± 0.002
BT-125-1	66	MC	0.95 ± 0.03
	66	TLD	0.90 ± 0.06
	55	Point (MCNP)	0.955 ± 0.005
	55	TLD	0.95 ± 0.07
	67	Point (MCNP)	0.955 ± 0.005
Syncor	This study	WAFAC	0.916 ± 0.002
PharmaSeed	This study	Point	0.958 ± 0.002
BT-125-2	55	Point (MCNP)	0.962 ± 0.005
	67	Point (MCNP)	0.967 ± 0.005

lated using the WAFAC voxel are probably more clinically relevant since this voxel size covers a solid angle comparable to the collimator of the WAFAC at NIST (Refs. 21 and 22) used for calibrating low-energy brachytherapy sources. Also included in the tables are dose rate constant values calculated or measured by other authors and TG-43 consensus values.

IV.A. Uncertainties

Uncertainties reported on dosimetry values calculated in this study are statistical uncertainties only. In general, statistical uncertainties on the dose rate constants are less than 0.3% for ^{125}I sources and less than 0.5% for ^{103}Pd sources. Statistical uncertainties on the radial dose function and anisotropy function for ^{125}I sources are less than 1% and 2% for distances from the source of $r_{seed} < r \leq 5$ cm and $5 < r \leq 10$ cm, respectively. For ^{103}Pd sources, statistical uncertainties on the radial dose function and anisotropy function are less than 2% and 3% for distances from the source of $r_{seed} < r \leq 5$ cm and $5 < r \leq 10$ cm, respectively.

Other sources of uncertainty in these calculations include uncertainties associated with voxel size, photon cross-section data, and source material and geometry definitions. As described in our previous study[12] we have attempted to minimize voxel size uncertainties by using very small scoring voxels for points near the source. Some sources of geometric uncertainty are variations in encapsulation thickness, end weld thickness, and the movement of internal source components. A full investigation of the effects of geometric uncertainty is beyond the scope of this study, however, they are discussed briefly below. For a more detailed analysis of the geometric uncertainties relevant to MC brachytherapy calculations, readers are referred to the studies by Dolan *et al.*,[23]

TABLE II. Dose rate constants Λ and uncertainties calculated in This study and from other authors for ^{103}Pd sources. See caption of Table I for details.

Manufacturer and seed name	Reference	Method	Λ cGy h^{-1} U^{-1}
BEBIG GmbH	This study	WAFAC	0.685 ± 0.002
IsoSeed	This study	Point	0.681 ± 0.005
Pd-103	68	Extrap. (PTRAN)	0.664 ± 0.017
	68	WAFAC (PTRAN)	0.660 ± 0.017
Best	This study	WAFAC	0.650 ± 0.002
Best Palladium-103	This study	Point	0.652 ± 0.002
2335	69	Point (PTRAN)	0.67 ± 0.02
	69	TLD	0.69 ± 0.06
	70	TLD	0.71 ± 0.07
	4	Consensus value	0.685
DRAXIMAGE	This study	WAFAC	0.632 ± 0.002
BrachySeed	This study	Point	0.632 ± 0.002
Pd-1	71	Point (MCNP)	0.65 ± 0.02
	71	TLD	0.63 ± 0.04
	73	Extrap (CYLTRAN)	0.613 ± 0.018
	72	TLD	0.66 ± 0.05
IBt	This study	WAFAC	0.669 ± 0.002
OptiSeed	This study	Point	0.670 ± 0.002
1032P	75	Point (MCNP)	0.712 ± 0.04
	75	TLD	0.720 ± 0.04
	76	Point (MCNP)	0.665 ± 0.01
	76	TLD	0.675 ± 0.05
IBt	This study	WAFAC	0.663 ± 0.002
InterSource	This study	Point	0.664 ± 0.002
1031L	74	Point (PTRAN)	0.696 ± 0.02
	74	TLD	0.664 ± 0.03
IsoAid.	This study	WAFAC	0.687 ± 0.002
Advantage	This study	Point	0.687 ± 0.002
IAPd-103A	77	Extrap (PTRAN)	0.70 ± 0.056
	77	TLD	0.69 ± 0.02
	78	Point (PTRAN)	0.71 ± 0.01
NASI	This study	WAFAC	0.650 ± 0.002
Prospera Pd-103	This study	Point	0.650 ± 0.002
Med3633	79	Extrap (MCNP)	0.672
	80	Extrap (PTRAN)	0.677
	84	TLD	0.702 ± 0.034
	3	Consensus value	0.688
Syncor	This study	WAFAC	0.671 ± 0.002
PharmaSeed	This study	Point	0.669 ± 0.002
BT-103-3	67	Point (MCNP)	0.659 ± 0.005
Theragenics	12	WAFAC	0.694 ± 0.002
TheraSeed	12	Point	0.772 ± 0.003
200	19	WAFAC (PTRAN)	0.691 ± 0.02
	19	Extrap (PTRAN)	0.797 ± 0.02
	85	TLD	0.680 ± 0.05
	3	Consensus value	0.686

Rivard,[58] Li,[56] and TG-43U1.[3] Combined uncertainties from voxel size effects, cross sections, and geometry are larger than the statistical uncertainties for the dosimetry parameters calculated in this study.

The study of the OncoSeed 6711 by Dolan *et al.*[23] shows that decreasing the Ti wall thickness of the 6711 seed by 14% results in a 2.4% increase in the dose rate to water at $r=1$ cm on the transverse axis. They report that the decrease does not effect the dose rate constant as there is a similar increase in the air kerma strength. This is consistent with calculations we performed for this study with the entire Ti encapsulation of the 6711 seed replaced with air. The lack of attenuation from the encapsulation resulted in a 35% increase in the dose rate to water at $r=1$ cm on the transverse axis but the dose rate constant was the same as that of the nominal calculation within statistical uncertainties. This calculation confirms the results of Dolan *et al.* and demonstrates that the thickness of the encapsulation wall is not a significant source of uncertainty in dose rate constant calculations.

In Sec. III, estimates of the extent of motion possible for internal source elements are provided. These values can be used to provide a rough estimate of the uncertainty introduced by this motion. For example, for a seed where the movement of a source element by 0.080 mm in the radial direction is possible (e.g., the OncoSeed 6711), if only $1/r^2$ effects are considered, then the range in values on the dose at 1 cm is 1.6% if the central rod is displaced the maximum distance towards or away from the dose point. Since the air-kerma strength is generally calculated at distances of 10 cm or more from the seed, the $1/r^2$ effects are close to negligible in this case and therefore the dose rate constant should also vary by an amount similar to the variation in dose at 1 cm. This estimate is likely an upper bound on the systematic uncertainty as evidenced by the detailed analysis of the OncoSeed 6711 by Dolan *et al.*[23] wherein they calculate a difference of 0.68% in both the dose to water at 1 cm and the dose rate constant when the central rod is displaced by a maximum of 0.080 mm in the radial direction. This uncertainty in the dose calculation will increase, possibly dramatically, for distances closer to the seed.

For most sources, this study is one of the first to extensively report dosimetry parameters at distances for $r<0.25$ cm. At these short distances, the internal position of the source elements can have a drastic effect on the dosimetry parameters. In Rivard's study of the Prospera Med3631 (Ref. 58) he shows that when the source elements are placed in the "diagonal" configuration (all seeds touching and resting against the source wall at one end of the encapsulation) there can be large differences in the anisotropy function when comparing one end of the source to the other. However, Rivard's study does not appear to account for the fact that, for example, the dose at $\theta=20°$ is potentially different from the dose at $\theta=340°$ (where $\theta=0°$ is defined to lie on the seed axis at the end closest to the source elements). It also does not appear that Rivard's study accounts for azimuthal variations of dose that will be present for configurations other than the ideal case. For example, for the diagonal configuration, the radial dose function depends on the azimuthal angle, ϕ, that it is calculated at.

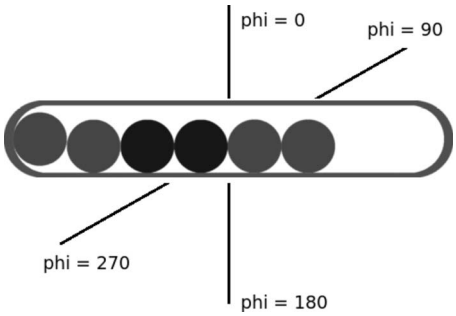

FIG. 1. Diagonal configuration of the ^{125}I Prospera Med3631 and ^{103}Pd Prospera Med3633 seeds as defined in Rivard's study of the Med3631 (see Ref. 58). Due to the asymmetries of this configuration the 2D TG-43 dosimetry parameters will depend on the azimuthal angle ϕ as well as the polar angle θ. Due to the azimuthal anisotropy the 2D TG-43 dosimetry protocol breaks down for sources like this, particularly for $r<0.25$ cm. Full Monte Carlo dosimetry calculations accounting for internal source positions would provide more accurate calculations of dose distributions.

To investigate the magnitude of this azimuthal dependence calculations were done for the Med3631 source in the diagonal configuration and compared with the ideal configurations. For the diagonal configuration the dose on the transverse axis at $r=0.25$ cm $\phi=0°$ (see Fig. 1) is approximately 8% lower then the dose at $r=0.25$ cm and $\phi=180°$. Similarly the dose at $r=0.25$ cm and $\phi=90°,270°$ is approximately 5% lower than at $\phi=0°$. At $r=1$ cm the doses at $\phi=0°$ and $\phi=90°,270°$, are respectively, 2% and 1% lower than the dose at $\phi=180°$. The azimuthal variation of dose at other polar angles are similar with, for example, 5% variations between $\phi=0°$ and $\phi=180°$ for $r=0.25$ cm and $\theta=25°$. Absolute dose differences between the two ends of the seed, however, can be very large. For example, the dose at $r=0.25$ cm and $\theta=25°$ is close to 300% higher than the dose at $r=0.25$ cm and $\theta=155°$. At $r=1$ cm this difference drops to 33%. For sources with such large azimuthal and polar anisotropies the two-dimensional (2D) TG-43 dosimetry protocol does not appear to be appropriate for calculating dose at small radii and points towards the need for full Monte Carlo treatment planning systems.

It should be noted that the statistical uncertainties on the calculated dosimetry parameters calculated in this study are frequently much lower than the uncertainties on previously reported data. This is especially true for values of the radial dose function and anisotropy function for distances greater than 5 cm from the source. For example, in Meigooni's study of the Best Pd-103 2335 (Ref. 69) source, the stated uncertainty on the radial dose function for distances greater than 5 cm is 5%. In this study the statistical uncertainty on the radial dose function for the same source is 0.7% at 7.5 cm from the source and reaches a maximum of 1.8% at a distance of 10 cm. Uncertainties on dose rate constants are also frequently much better than currently available values. TG-43U1 recommends assigning a systematic uncertainty of approximately 2.5% attributed to cross section data, seed ge-

ometry and photon spectra. This means that the statistical uncertainties on dose rate constants in this study are mostly negligible for both ^{125}I and ^{103}Pd sources. Thus, dose rate constants can be assumed to have a maximum total uncertainty of approximately 2.5%, which in some cases is 20%–50% lower than the stated uncertainty on previously calculated Monte Carlo values.

IV.B. Comparison to published data

Due to the large amount of data it is not practical to do a detailed comparison of all of the dosimetry data available from this study and studies by other authors for all sources. Instead this section highlights a few differences which can not readily be explained by statistical uncertainties. In the following discussion, absolute uncertainties on the least significant digit of dose rate constants are given in brackets following the value. Detailed comparisons between our data and other authors' data for the STM ^{125}I seed, Imagyn IsoStar seed, and Theragenics model 200 ^{103}Pd seed are available in our preceding article.[12]

The Amersham 6733 EchoSeed was previously studied by Sowards and Meigooni.[29] In their study the dose rate constant is calculated using an air kerma strength calculated at a point 5 cm from the source. This source contains radioactive ^{125}I coated on a right circular cylinder which has been shown to lead to variations in the air-kerma strength depending on the voxel size used for scoring.[17–19] Solberg and Meigooni found a value of $\Lambda=0.97(3)$ cGy h^{-1} U^{-1} [where the (3) indicates the absolute uncertainty on the least significant digit, i.e., $\Lambda=0.97\pm0.03$ cGy h^{-1} U^{-1}] for the dose rate constant, while in this study, using the methods described above, the dose rate constant is calculated to be $\Lambda=0.929(2)$ cGy h^{-1} U^{-1} and $\Lambda=0.947(3)$ cGy h^{-1} U^{-1} using the WAFAC and point voxels, respectively. Since the WAFAC voxel value is more appropriate, this implies our calculated value is 4.4% lower than the TG-43 MC value and 5.4% less than the consensus value.

The Braquibac seed shows a 3.5% variation in the dose rate constant calculated using different voxel sizes for scoring air-kerma strength because it contains a right circular cylindrical source element. Pirchio *et al.*[31] published a value of $\Lambda=0.937(4)$ cGy h^{-1} U^{-1} for the dose rate constant based on an extrapolation of the air-kerma strength along the transverse axis.[31] The value from Pirchio *et al.*[31] is 1.2% lower and 2.2% greater than the values of $\Lambda=0.949(3)$ cGy h^{-1} U^{-1} and $\Lambda=0.917(3)$ cGy h^{-1} U^{-1} calculated in this study using the point and WAFAC voxels, respectively. This means our best calculation of the dose rate constant is 2.2% lower than the only dose rate constant currently available for this source.

Sowards and Meigooni's study of the Best 2301 ^{125}I source used a cylindrical encapsulation and cylindrical tungsten marker to model the seed geometry.[35] In our model we have used hemispherical shells for the end cap and added hemispherical ends to the tungsten marker in order to reflect the diagram of the 2301 seed presented in the TG-43U1 report. These differences led to some discrepancies between the anisotropy data calculated in this study and Sowards and Meigooni's study. In general our calculated anisotropy function values tend to agree slightly better with the TLD measurements made by Nath and Yue.[37]

In Rivard's MC study of the IPlant 3500 ^{125}I source[50] a dose rate constant value of $\Lambda=1.017(5)$ cGy h^{-1} U^{-1} was obtained. However, the cross sections used in that study are now considered to be outdated.[3] The dose rate constants obtained in this study are 2.3% lower at $\Lambda=0.994(2)$ cGy h^{-1} U^{-1}. In this study the radial dose function at 5 cm is approximately 10% lower than the value calculated by Rivard. However, our radial dose function generally agrees within 2.0% with the values calculated by Duggan and Johnson[51] which have been adopted as the TG-43 consensus values.[4] Duggan and Johnson's Monte Carlo study[51] does not include a dose rate constant calculation.

The IsoAid Advantage ^{125}I source has been studied by Meigooni *et al.*[54] and Solberg *et al.*[55] The model in Solberg *et al.* has end welds of 0.250 mm thickness while Meigooni's model has welds of 0.100 mm thickness. In this study we chose to use the same end weld thickness as Meigooni *et al.* The anisotropy function calculated in this study agrees reasonably well with Meigooni's data for angles greater than 15°, however, there are differences in the anisotropy function on the order of 20% for angles less than 10°. Our dose rate constants and radial dose function data beyond 2 cm are also significantly lower (10% at 5.0 cm) than the values calculated by Meigooni *et al.* These differences can likely be explained by the fact that the study by Meigooni *et al.*[54] used the DLC-99 photon cross sections which are now considered outdated.[3] Our radial dose function agrees much better with the values calculated by Solberg *et al.*[55] who used the XCOM photoelectric cross sections. The Advantage ^{125}I is also a source containing a cylinder coated in radioactive material which in this case causes the dose rate constant to vary by 3.5% depending on the size of the voxel used for scoring air kerma. Solberg *et al.* based their dose rate constant calculation on an air-kerma strength calculated in a small voxel 50 cm from the source. As expected their calculated value of $\Lambda=0.962(5)$ cGy h^{-1} U^{-1} agrees well with the value of $\Lambda=0.959(2)$ cGy h^{-1} U^{-1} calculated in this study using the point voxel, but is 4.0% higher than the value of $\Lambda=0.925(2)$ cGy h^{-1} U^{-1} calculated using the WAFAC voxel. As discussed above, the latter value is the preferred which means our best value is 5.9% less than Meigooni's value of $\Lambda=0.98(3)$ cGy h^{-1} U^{-1} and 5.5% less than the consensus value.

The dose rate constant of the Med3631 ^{125}I source calculated in this study is $\Lambda=0.978(2)$ cGy h^{-1} U^{-1} which is 3.4% less than the value calculated by Rivard[58] with the outdated DLC-189 cross sections. The radial dose function in this study is also 7.8% higher than the TLD measured[59] TG-43U1[3] consensus value at a distance of 5.0 cm from the source.

In their study of the SelectSeed Karaiskos *et al.* gave a value of $\Lambda=0.954(5)$ cGy h^{-1} U^{-1} for the dose rate constant

based on an extrapolation of the air-kerma strength along the transverse axis.[61] As is the case for other seeds containing a cylindrical source element, the SelectSeed shows a variation in the calculated dose rate constant depending on the voxel size used for scoring air kerma. The calculation by Karaiskos *et al.* is 1.1% and 4.0% greater than the values of $\Lambda=0.944(3)$ cGy h^{-1} U^{-1} and $\Lambda=0.917(2)$ cGy h^{-1} U^{-1} calculated in this study using the point and WAFAC voxels, respectively. Thus, our best calculation of the dose rate constant is 3.7% lower than the only other MC dose rate constant currently available for this source.

As with the Best 2301 ^{125}I source, our model of the Best 2335 ^{103}Pd source had an encapsulation with hemispherical shells on the ends rather than a cylinder as used in the study by Meigooni *et al.*.[69] In general our anisotropy function data are much smoother and show less nonphysical fluctuation than the data published by Meigooni *et al.* The calculated dose rate constant of $\Lambda=0.650(2)$ cGy h^{-1} U^{-1} in this study is also approximately 3.1% lower than Meigooni *et al.*'s value of $\Lambda=0.67(2)$ cGy h^{-1} U^{-1} which may only reflect our lower statistical uncertainties.

The dose rate constant value of $\Lambda=0.633(2)$ cGy h^{-1} U^{-1} calculated in this study for the DRAXIMAGE Pd-1 source is 2.7% lower than the value of $\Lambda=0.65(2)$ cGy h^{-1} U^{-1} calculated by Meigooni *et al.*[71] using PTRAN and 3.1% higher than the value of $\Lambda=0.61(2)$ cGy h^{-1} U^{-1} calculated by Chan and Prestwich[73] using CYLTRAN. The radial dose function calculated in this study agrees well with the data by Chan and Prestwich and is 20% lower than the radial dose function calculated by Meigooni *et al.* at 5 cm. Anisotropy function values calculated in this study are lower by 5%–10% when compared to the Chan and Prestwich data set for distances less than 1 cm from the source but generally agree within 5% at a distance of 5 cm from the source.

As described in Sec. V, comparisons of radial dose function and anisotropy function data calculated in this study with data calculated by other authors are provided in a graphical form on the CLRP TG-43 web resource for all sources.

V. WEB RESOURCE

As part of this study the Carleton Laboratory for Radiotherapy Physics TG-43 Parameter Database website[83] has been created. The website includes a separate web page for each brachytherapy seed. The content of an individual seed page is as follows; a to-scale drawing and description of the materials and seed geometry used in these calculations, a full set of tabulated dosimetry data, a graphical representation of the dosimetry data which includes comparisons with data calculated by other authors and references and links to relevant published papers. The dosimetry data on the web site includes the values of the dose rate constants calculated in this study and in studies by other authors. It also includes radial dose functions and anisotropy data. Radial dose functions are tabulated at intervals of 0.01 cm for $0.05\leqslant r\leqslant 0.1$ cm, 0.1 cm for $0.1<r\leqslant 1.0$ cm, and 0.5 cm for $5<r\leqslant 10$ cm. Fit coefficients from our accompanying study on radial dose function fitting[82] are also provided for each source. Anisotropy function data are tabulated at 32 polar angles from 0° to 90° with a minimum resolution of 5° and higher resolution for angles closer to the transverse and seed axis. Anisotropy functions and anisotropy factors are tabulated at 12 different radii from 0.1 to 10 cm. Relative statistical uncertainties are also provided for all of the data presented on the website. For the user's convenience, the tabulated dosimetry data are available in HTML tables and spread-sheets. A description of the calculation methods used in this study and theBrachyDose Monte Carlo code are also available on the site. Dosimetry data for more sources will be added to the website as they become available.

VI. CONCLUSION

In this study the previously benchmarked[12] EGSnrc usercode BrachyDose is used to calculate a complete set of TG-43 dosimetry data for a total of 27 low-energy photon emitting brachytherapy sources (18 ^{125}I and 9 ^{103}Pd sources). This data set is unique due to the fact that the TG-43 data for all of the sources are generated using a consistent set of methods for all of the sources included. Calculations included state-of-the-art XCOM photon cross sections, detailed source geometry models, and dosimetry data often with much better statistical precision, higher resolution, and greater spatial extent than is currently available in the literature for many of these sources. For most of the seeds this is the first study to report anisotropy function values for distances less than 0.5 cm from the source which should be of particular interest to centers doing eye plaque brachytherapy dosimetry. More study is required to fully assess the impact of geometric uncertainties at points less than 0.25 cm from the source. It is found that dealing with the effects of asymmetric geometries in the seeds is virtually impossible within the essentially two-dimensional formalism of TG-43. If these asymmetry effects are important, they will need to be handled using a Monte Carlo calculation of the complete dose distribution of the multiseed implant. The complete set of dosimetry data calculated in this study are made available via a website (see Ref. 83). Subject to availability of resources, the web pages will be updated as manufactures introduce new brachytherapy sources and designs including seeds using other low-energy photon emitting isotopes such as ^{131}Cs.

ACKNOWLEDGMENTS

The authors would like to thank Gultekin Yegin at Celal Bayar University in Turkey for his ongoing collaboration on the development of the BrachyDose code. They wish to acknowledge Dr. Ali Meigooni for his assistance in clarifying some source geometry definitions as well as Elsayed Ali and Dan La Russa for their helpful comments regarding this article. We thank Jose Perez-Calatayud for thought provoking discussions regarding normalizing $g(r)$ data. Some of the calculations in this study have made use of WestGrid computing resources, which are funded in part by the Canada Founda-

tion for Innovation, Alberta Innovation and Science, BC Advanced Education, and the participating research institutions. This work is also partially funded by the Canada Foundation for Innovation, the Ontario Innovation Trust, NSERC, The Canada Research Chair's program, and Varian, Inc.

[a]Electronic mail: rtaylor@physics.carleton.ca
[b]Electronic mail: drogers@physics.carleton.ca

[1]Radiological Physics Center, The joint AAPM/RPC registry of brachytherapy sources, The M.D. Anderson Cancer Center, Houston, Texas; see http://rpc.mdanderson.org/rpc/.
[2]R. Nath, L. L. Anderson, G. Luxton, K. A. Weaver, J. F. Williamson, and A. S. Meigooni, "Dosimetry of interstitial brachytherapy sources: Recommendations of the AAPM Radiation Therapy Committee Task Group No. 43," Med. Phys. **22**, 209–234 (1995).
[3]M. J. Rivard, B. M. Coursey, L. A. DeWerd, M. S. Huq, G. S. Ibbott, M. G. Mitch, R. Nath, and J. F. Williamson, "Update of AAPM Task Group No. 43 Report: A revised AAPM protocol for brachytherapy dose calculations," Med. Phys. **31**, 633–674 (2004).
[4]M. J. Rivard, W. M. Butler, L. A. DeWerd, M. S. Huq, G. S. Ibbott, A. S. Meigooni, C. S. Melhus, M. G. Mitch, R. Nath, and J. F. Williamson, "Supplement to the 2004 update of the AAPM Task Group No. 43 Report," Med. Phys. **34**, 2187–2205 (2007).
[5]J. F. Williamson, "Comparison of measured and calculated dose rates in water near I-125 and Ir-192 seeds," Med. Phys. **18**, 776–786 (1991).
[6]J. F. Williamson, "Monte Carlo evaluation of kerma at a point for photon transport problems," Med. Phys. **14**, 567–576 (1987).
[7]*MCNP—A general Monte Carlo N-particle Transport Code Version 5*, Report LA-UR-03-1987, edited by F. B. Brown (Los Alamos National Laboratory, Los Alamos, NM, 2003).
[8]I. Kawrakow, "Accurate condensed history Monte Carlo simulation of electron transport. I. EGSnrc, the new EGS4 version," Med. Phys. **27**, 485–498 (2000).
[9]I. Kawrakow and D. W. O. Rogers, *The EGSnrc Code System: Monte Carlo simulation of Electron and Photon Transport*, Technical Report PIRS-701 (National Research Council of Canada, Ottawa, Canada, 2000).
[10]G. Yegin and D. W. O. Rogers, "A fast Monte Carlo code for multi-seed brachytherapy treatments including interseed effects," Med. Phys. **31**, 1771 (abs) (2004).
[11]G. Yegin, R. E. P. Taylor, and D. W. O. Rogers, "BrachyDose: An EGSnrc user-code for full Monte Carlo simulation of brachytherapy implants using CT data," unpublished.
[12]R. E. P. Taylor, G. Yegin, and D. W. O. Rogers, "Benchmarking BrachyDose: Voxel-based EGSnrc Monte Carlo calculations of TG-43 dosimetry parameters," Med. Phys. **34**, 445–457 (2007).
[13]G. Yegin, "A new approach to geometry modelling of Monte Carlo particle transport: an application to EGS," Nucl. Instrum. Methods Phys. Res. B **211**, 331–338 (2003).
[14]M. J. Berger and J. H. Hubbell, XCOM: Photon Cross Sections on a Personal Computer, Report NBSIR87–3597, NIST, Gaithersburg, MD 20899, 1987.
[15]J. F. Williamson and M. J. Rivard, "Quantitative dosimetry methods for brachytherapy," in *Brachytherapy Physics*, edited by B. R. Thomadsen, M. J. Rivard, and W. M. Butler (Medical Physics, Madison, WI, 2005), pp. 233–294.
[16]I. Kawrakow, "On the effective point of measurement in megavoltage photon beams," Med. Phys. **33**, 1829–1839 (2006).
[17]J. F. Williamson, "Monte Carlo modeling of the transverse-axis dose distribution of the Model 200 ^{103}Pd interstitial brachytherapy source," Med. Phys. **27**, 643–654 (2000).
[18]A. S. Kirov and J. F. Williamson, "Monte Carlo-aided dosimetry of the Source Tech Medical model STM1251 I-125 interstitial brachytherapy source," Med. Phys. **28**, 764–772 (2001).
[19]J. I. Monroe and J. F. Williamson, "Monte Carlo-aided dosimetry of the Theragenics TheraSeed model 200 ^{103}Pd interstitial brachytherapy seed," Med. Phys. **29**, 609–621 (2002).
[20]G. Lymperopoulou, P. Papagiannis, A. Angelopoulos, L. Sakelliou, P. Karaiskos, P. Sandilos, A. Przykutta, and D. Baltas, "Monte Carlo and thermoluminescence dosimetry of the new IsoSeed model I125.S17 ^{125}I interstitial brachytherapy seed," Med. Phys. **32**, 3313–3317 (2005).
[21]R. Loevinger, "Wide-angle free-air chamber for calibration of low-energy brachytherapy sources," Med. Phys. **20**, 907 (1993).
[22]S. M. Seltzer, P. J. Lamperti, R. Loevinger, M. G. Mitch, J. T. Weaver, and B. M. Coursey, "New national air-kerma-strength standards for ^{125}I and ^{103}Pd brachytherapy Seeds," J. Res. Natl. Inst. Stand. Technol. **108**, 337–358 (2003).
[23]J. Dolan, Z. Li, and J. F. Williamson, "Monte Carlo and experimental dosimetry of an ^{125}I brachytherapy seed," Med. Phys. **33**, 4675–4684 (2006).
[24]J. F. Williamson and F. J. Quintero, "Theoretical evaluation of dose distributions in water models 6711 and 6702 ^{125}I seeds," Med. Phys. **15**, 891–897 (1988).
[25]J. F. Williamson, "Monte Carlo evaluation of specific dose constants in water for ^{125}I seeds," Med. Phys. **15**, 686–694 (1988).
[26]E. Mainegra, R. Capote, and E. Lopez, "Dose rate constants for ^{103}Pd, ^{125}I, ^{196}Yb, ^{192}Ir, brachytherapy sources: An EGS4 Monte Carlo study," Phys. Med. Biol. **43**, 1557–1566 (1998).
[27]E. Mainegra, R. Capote, and E. Lopez, "Radial dose functions for ^{103}Pd, ^{125}I, ^{196}Yb, ^{192}Ir, brachytherapy sources: An EGS4 Monte Carlo study," Phys. Med. Biol. **45**, 703–717 (2000).
[28]R. Capote, E. Mainegra, and E. Lopez, "Anisotropy functions for low energy interstitial brachytherapy sources: An EGS4 Monte Carlo study," Phys. Med. Biol. **46**, 135–150 (2001).
[29]K. Sowards and A. S. Meigooni, "A Monte Carlo evaluation of the dosimetric characteristics of the EchoSeed™ model 6733 ^{125}I brachytherapy source," Brachytherapy **1**, 227–232 (2002).
[30]A. S. Meigooni, S. A. Dini, K. Sowards, J. L. Hayes, and A. Al-Otoom, "Experimental determination of the TG-43 dosimetric characteristics of EchoSeed model 6733 ^{125}I brachytherapy source," Med. Phys. **29**, 939–942 (2002).
[31]R. Pirchio, E. Galiano, M. Saravi, D. Banchik, and C. Muñoz, "On the physical, spectra, and dosimetric characteristics of a new ^{125}I brachytherapy source," Med. Phys. **34**, 2801–2806 (2007).
[32]H. Hedtjärn, G. A. Carlsson, and J. F. Williamson, "Monte Carlo-aided dosimetry of the symmetra model I25.S06 I^{125}, interstitial brachytherapy seed," Med. Phys. **27**, 1076–1085 (2000).
[33]N. S. Patel, S.-T. Chiu-Tsao, J. F. Williamson, P. Fan, T. Duckworth, D. Shasha, and L. B. Harrison, "Thermoluminescent dosimetry of the Symmetra ^{125}I model I25.S06 interstitial brachytherapy seed," Med. Phys. **28**, 1761–1769 (2001).
[34]E. Pantelis, D. Baltas, E. Georgiou, P. Karaiskos, G. Lymperopoulou, P. Papariannis, L. Sakelliou, I. Seimenis, and E. Stilliaris, "Dose characterization of the new Bebig IsoSeed I25.S17 using polymer gel and MRI," Nucl. Instrum. Methods Phys. Res. A **569**, 529–532 (2006).
[35]K. Sowards and A. S. Meigooni, "A Monte Carlo evaluation of the dosimetric characteristics of the Best model 2301 ^{125}I brachytherapy source," Brachytherapy **57**, 327–333 (2002).
[36]A. S. Meigooni, D. M. Gearheart, and K. Sowards, "Experimental determination of dosimetric characteristics of Best ^{125}I brachytherapy source," Med. Phys. **27**, 2168–2173 (2000).
[37]R. Nath and N. Yue, "Dosimetric characterization of an encapsulated interstitial brachytherapy source of ^{125}I on a tungsten substrate," Brachytherapy **1**, 102–109 (2002).
[38]J. F. Williamson, "Dosimetric characteristics of the DRAXIMAGE model LS-1 interstitial brachytherapy source design: A Monte Carlo investigation," Med. Phys. **29**, 509–521 (2002).
[39]R. Wang and R. Sloboda, "Monte Carlo dose parameters of the BrachySeed model LS-1 ^{125}I brachytherapy source," Appl. Radiat. Isot. **56**, 805–813 (2002).
[40]G. Chan and W. V. Prestwich, "Dosimetric properties of the new ^{125}I BrachySeed model LS-1 source," Med. Phys. **29**, 190–200 (2002).
[41]G. H. Chan, R. Nath, and J. F. Williamson, "On the development of consensus values of reference dosimetry parameters for interstitial brachytherapy sources," Med. Phys. **31**, 1040–1045 (2004).
[42]R. Nath and N. Yue, "Experimental determination of a newly designed encapsulated interstitial brachytherapy source of iodine-125-model LS-1 BrachySeed," Appl. Radiat. Isot. **55**, 813–821 (2001).
[43]A. S. Meigooni, M. M. Yoe-Sein, A. Y. Al-Otoom, and K. Sowards, "Determination of the dosimetric characteristics of InterSource ^{125}I brachytherapy source," Appl. Radiat. Isot. **56**, 589–599 (2002).
[44]B. Reniers, S. Vynckier, and P. Scalliet, "Dosimetric study of the new InterSource^{125} iodine seed," Med. Phys. **28**, 2285–2299 (2001).
[45]M. J. Rivard, W. M. Butler, L. A. DeWerd, M. S. Huq, G. S. Ibbott, C. S. Melhus, M. G. Mitch, R. Nath, and J. J. Williamson, "Response to "Com-

ment on 'Update of AAPM Task Group No. 43 Report: A revised AAPM protocol for brachytherapy dose calculations," Med. Phys. **32**, 1822–1824 (2005).
[46]D. M. Gearheart, A. Drogin, K. Sowards, A. Meigooni, and G. S. Ibbott, "Dosimetric characteristics of a new ^{125}I brachytherapy source," Med. Phys. **27**, 2278–2285 (2000).
[47]R. Nath and N. Yue, "Dose distribution along the transverse axis of a new ^{125}I source for interstitial brachytherapy," Med. Phys. **27**, 2536–2540 (2000).
[48]G. S. Ibbott and R. Nath, "Dose-rate constant for Imagyn ^{125}I brachytherapy source," Med. Phys. **28**, 705 (2001).
[49]G. S. Ibbott, "Monte Carlo determination of dose rate constant," Med. Phys. **29**, 1637–1638 (2002).
[50]M. J. Rivard, "Comprehensive Monte Carlo calculations of AAPM Task Group Report No. 43 dosimetry parameters for the model 3500 I-Plant ^{125}I brachytherapy source," Appl. Radiat. Isot. **57**, 381–389 (2002).
[51]D. Duggan and B. L. Johnson, "Improved radial dose function estimation using current version MCNP Monte Carlo simulation: Model 6711 and ISC3500 125I brachytherapy sources," Appl. Radiat. Isot. **61**, 1443–1450 (2004).
[52]D. Duggan and B. L. Johnson, "Dosimetry of the I-Plant model 3500 iodine-125 brachytherapy source," Med. Phys. **28**, 661–670 (2001).
[53]R. E. Wallace, "Model 3500 ^{125}I brachytherapy source dosimetric characterization," Appl. Radiat. Isot. **56**, 581–587 (2001).
[54]A. S. Meigooni, J. L. Hayes, H. Zhang, and K. Sowards, "Experimental and theoretical determination of dosimetric characteristics of IsoAid ADVANTAGE^{TM} ^{125}I brachytherapy source," Med. Phys. **29**, 2152–2158 (2002).
[55]T. D. Solberg, J. J. DeMarco, G. Hugo, and R. E. Wallace, "Dosimetric parameters of three new solid core I-125 brachytherapy sources," J. Appl. Clin. Med. Phys. **3**, 119–134 (2002).
[56]Z. Li, "Monte Carlo calculations of dosimetry parameters of the Urocor Prostaseed ^{125}I source," Med. Phys. **29**, 1029–1034 (2002).
[57]R. E. Wallace, "Empirical dosimetric characterization of model I125-SL ^{125}Iodine brachytherapy source in phantom," Med. Phys. **27**, 2796–2802 (2000).
[58]M. J. Rivard, "Monte Carlo calculations of AAPM Task Group Report No. 43 dosimetry parameters for the MED3631-A/M ^{125}I source," Med. Phys. **28**, 629–637 (2001).
[59]Z. Li, J. J. Fan, and J. R. Palta, "Experimental measurements of dosimetric parameters on the transverse axis of a new ^{125}I source," Med. Phys. **27**, 1275–1280 (2000).
[60]R. E. Wallace and J. J. Fan, "Report on the dosimetry of a new design ^{125}Iodine brachytherapy source," Med. Phys. **26**, 1925–1931 (1999).
[61]P. Karaiskos, P. Papagiannis, L. Sakelliou, G. Anagnostopoulos, and D. Baltas, "Monte Carlo dosimetry of the selectSeed ^{125}I interstitial brachytherapy seed," Med. Phys. **28**, 1753–1760 (2001).
[62]G. Anagnostopoulos, D. Baltas, P. Karaiskos, P. Sandilos, P. Papagiannis, and L. Sakelliou, "Thermoluminescent dosimetry of the selectSeed ^{125}I interstitial brachytherapy seed," Med. Phys. **29**, 709–716 (2002).
[63]P. Papagiannis, L. Sakelliou, G. Anagnostopoulos, and D. Baltas, "On the dose rate constant of the selectSeed ^{125}I interstitial brachytherapy seed," Med. Phys. **33**, 1522–1523 (2006).
[64]S. Chiu-Tsao, T. L. Duckworth, C. Hsiung, Z. Li, J. Williamson, N. Patel, and L. B. Harrison, "Thermoluminescent dosimetry of the SourceTech Medical model STM1251 ^{125}I seed," Med. Phys. **30**, 1735–1732 (2003).
[65]Z. Li and J. F. Williamson, "Measured transverse-axis dosimetric parameters of the model STM1251 ^{125}I interstitial source," J. Appl. Clin. Med. Phys. **3**, 212–217 (2002).
[66]C. C. Popescu, J. Wise, K. Sowards, A. S. Meigooni, and G. S. Ibbott, "Dosimetric characteristics of the PharmaSeed model BT-125-1 source," Med. Phys. **27**, 2174–2181 (2000).
[67]J. J. DeMarco, G. Hugo, and T. D. Solberg, "Dosimetric characteristics for three low-energy brachytherapy sources using the Monte Carlo N-Particle code," Med. Phys. **29**, 662–668 (2002).
[68]G. M. Daskalov and J. F. Williamson, "Monte Carlo-aided dosimetry of the new Bebig IsoSeed ^{103}Pd interstitial brachytherapy seed," Med. Phys. **28**, 2154–2161 (2001).
[69]A. S. Meigooni, Z. Bharucha, M. Yoe-Sein, and K. Sowards, "Dosimetric characteristics of the Best double-wall ^{103}Pd brachytherapy source," Med. Phys. **28**, 2567–2575 (2001).
[70]S. W. Peterson and B. Thomadsen, "Measurements of the dosimetric constants for a new ^{103}Pd brachytherapy source," Brachytherapy **1**, 110–119 (2002).
[71]A. S. Meigooni, H. Zhang, C. Perry, S. A. Dini, and R. A. Koona, "Theoretical and experimental determination of dosimetric characteristics for brachyseed Pd-103, model Pd-1, source," Appl. Radiat. Isot. **58**, 533–541 (2003).
[72]R. Nath, N. Yue, and E. Roa, "Experimental determination of dosimetric characterization of a newly designed encapsulated interstitial brachytherapy source of ^{103}Pd-model Pd-1," Med. Phys. **29**, 2433–2434 (2002).
[73]G. Chan and W. V. Prestwich, "Monte Carlo investigation of the dosimetric properties of the new ^{103}Pd BrachySeed model Pd-1 source," Med. Phys. **29**, 1984–1990 (2002).
[74]A. S. Meigooni, K. Sowards, and M. Soldano, "Dosimetric characteristics of InterSource^{103} palladium brachytherapy source," Med. Phys. **27**, 1093–1100 (2000).
[75]S. Bernard and S. Vynckier, "Dosimetric study of a new polymer encapsulated ^{103}Pd seed," Phys. Med. Biol. **50**, 1493–1504 (2005).
[76]Z. Wang and N. Hertel, "Determination of dosimetric characteristics of OptiSeed a plastic brachytherapy ^{103}Pd source," Appl. Radiat. Isot. **63**, 311–321 (2005).
[77]A. S. Meigooni, S. Dini, K. Dou, S. Awan, and G. Gopalakrishnan, "Experimental and Monte Carlo dosimetric characterization of ADVANTAGE ^{103}Pd," Appl. Radiat. Isot. **64**, 881–887 (2006).
[78]K. Sowards, "Monte Carlo dosimetric characterization of the IsoAid ADVANTAGE ^{103}Pd brachytherapy source," J. Appl. Clin. Med. Phys. **8**, 18–25 (2007).
[79]M. J. Rivard, "A discretized approach to determining TG-43 brachytherapy dosimetry parameters: Case study using Monte Carlo calculations for the MED3633 ^{103}Pd source," Appl. Radiat. Isot. **55**, 775–782 (2001).
[80]Z. Li, J. R. Palta, and J. J. Fan, "Monte Carlo caculations and experimental measurements of dosimetry parameters of a new ^{103}Pd source," Med. Phys. **27**, 1108–1112 (2000).
[81]Z. Chen and R. Nath, "Dose rate constant and energy spectrum of interstitial brachytherapy sources," Med. Phys. **28**, 86–96 (2001).
[82]R. E. P. Taylor and D. W. O. Rogers, "More accurate fitting of ^{125}I and ^{103}Pd radial dose functions," Med. Phys. **35**, 4242–4250 (2008).
[83]R. E. P. Taylor and D. W. O. Rogers, "The Carleton Laboratory for Radiotherapy Physics TG-43 Parameter Database," http://www.physics.carleton.ca/clrp/seed_database/.
[84]R. E. Wallace and J. J. Fan, "Dosimteric characterization of a new design ^{103}Pd brachytherapy source," Med. Phys. **26**, 2465–2470 (1999).
[85]R. Nath, N. Yue, K. Shahnazi, and P. Bongiorini, "Measurement of dose-rate constant for ^{103}Pd seeds with air kerma strength calibration based upon a primary national standard," Med. Phys. **27**, 655–658 (2000).